Electronic Journal of Education, Social Economics and Technology
Vol. 7, No. 1, (2026), e1514
ISSN 2723-6250 (online)
DOI: https://doi.org/10.33122/ejeset.v7i1.1514

Research Article

Interfacial Wave Dynamics and Liquid Holdup During Slug-to-Annular Transition in Horizontal Air-Water Two-Phase Flow Using Conductivity-Based Measurements

Suryadi, Muhammad Sayuthi, M. Iqbal Adhya Putra, Muhammad Habibi, Aljufri

Mechanical Engineering Study Program, Universitas Malikussaleh, Aceh Utara, 24351, Indonesia
*Corresponding Author: suryadi80@unimal.ac.id | Phone: +6285228557636

ABSTRACT

Two-phase water–air flow in a horizontal pipe exhibits complex characteristics due to the interaction of superficial velocity, gravity, surface tension and interface dynamics. This study aims to analyse the wave characteristics and liquid hold-up during the slug–annular transition in co-current water–air flow. Experiments were conducted using a horizontal acrylic pipe with an internal diameter of 26 mm and a development length of 9.5 m. Flow patterns were observed using a high-speed camera at 400 frames per second, whilst liquid hold-up was measured using three Constant Electric Current Method (CECM) sensors spaced 215 mm apart. Signals were recorded at a sampling rate of 500 Hz for 20 s and analysed using statistical methods and Power Spectral Density (PSD). The results show that an increase in the superficial velocity of both the gas and liquid influences wave development and the formation of the liquid film towards an annular pattern. The wave velocity increases as the superficial velocity of both the gas and liquid rises. Under annular conditions, ripple waves and disturbance waves were identified, indicating fluctuations in the liquid film. The average liquid hold-up increased with increasing liquid superficial velocity at a constant gas velocity. The combination of visualisation and CECM is effective for characterising interface dynamics and liquid hold-up distribution during the slug–annular transition.

Keywords: Two-Phase Flow; Slug–Annular Transition; Annular Flow; Liquid Hold-Up; CECM; PSD

1. INTRODUCTION

Gas liquid two-phase flow is fundamental to numerous engineering systems, including oil and gas transportation, geothermal facilities, nuclear reactors, boilers, condensers, refrigeration systems, and chemical-processing equipment. Unlike single-phase flow, two-phase flow involves strong interfacial interactions, phase slip, non-uniform phase distribution, and significant fluctuations in pressure and liquid holdup. These interactions produce distinct flow patterns whose characteristics depend on superficial velocities, fluid properties, pipe diameter, surface tension, gravity, and pipe orientation [1–5]. Recent experimental studies confirm that flow-pattern transitions are strongly dependent on the combined effects of inertial, gravitational, viscous, and interfacial forces rather than on a single governing parameter (Zdornikov, S. A., Isaenkov, S. V., & Cherdantsev, A. V. (2024).

For horizontal gas–liquid flow, the principal regimes include bubbly, stratified, stratified-wavy, plug, slug, and annular flow. Among these, annular flow is particularly important because it develops at relatively high gas superficial velocity, when the gas forms a continuous core and the liquid is transported as a film along the pipe wall. In horizontal pipes, gravitational effects produce a strongly asymmetric liquid-film distribution, with greater film accumulation generally occurring near the pipe bottom [1,2,7]. Recent experiments demonstrate that the transition from stratified to annular flow can occur progressively downstream and may be established even before fully developed disturbance waves appear [Zdornikov, S. A., Isaenkov, S. V., & Cherdantsev, A. V. (2026)]. Moreover, liquid viscosity and surface tension can substantially modify the conditions required for liquid-film lifting and annular-flow formation [2].

The complexity of two-phase flow has motivated the development of several flow-pattern maps and mechanistic models. Although classical maps remain useful as engineering references, their applicability can be limited when fluid properties, pipe dimensions, or operating conditions differ substantially from the original experimental databases. Recent studies have therefore emphasized experimental characterization and data-driven approaches for flow-pattern identification [Nie, F., Wang, H., Song, Q., Zhao, Y., Shen, J., & Gong, M. (2022). Image-based convolutional neural networks, support-vector machines, recurrence analysis, and other signal-processing methods have demonstrated considerable potential for objectively identifying complex two-phase flow structures [Amirsoleymani, A., Ting, D. S.-K., Carriveau, R., Brown, D., & McGillis, A. (2023)]. These approaches are particularly relevant because conventional visual classification may be subjective and may not adequately capture transient interfacial dynamics.

Annular flow is characterized by a thin base liquid film, superimposed disturbance waves and ripples, and, under sufficiently high gas velocity, entrained droplets in the gas core. These structures govern momentum transfer, pressure drop, liquid entrainment, heat transfer, and mass transfer [Zhang, H., Umehara, Y., Yoshida, H., & Mori, S. (2023)]. Recent measurements using conductance sensors, laser-induced fluorescence, and other non-intrusive techniques have demonstrated that liquid-film thickness is highly dynamic and varies significantly in both the axial and circumferential directions [Zhang, H., Umehara, Y., Yoshida, H., & Mori, S. (2023)]. In particular, disturbance waves may originate near the bottom of a horizontal pipe and subsequently propagate and spread circumferentially along the wetted wall [1,3].

The development of disturbance waves is therefore a critical component of annular-flow dynamics. Experimental investigations have shown that disturbance-wave velocity, frequency, amplitude, and wavelength depend on gas and liquid flow rates, surface tension, density ratio, liquid-film thickness, and droplet entrainment [13–17]. The influence of entrained droplets is particularly important because droplet–film exchange modifies the gas-core properties and the interfacial shear stress, thereby affecting disturbance-wave propagation [16,17]. Recent modeling studies have incorporated disturbance waves as an additional flow field and demonstrated that non-equilibrium wave development must be considered when describing developing annular flows [18]. For horizontal annular flow, gravitational asymmetry introduces an additional level of complexity. High-resolution measurements using Brightness-Based Laser-Induced Fluorescence (BBLIF) have revealed that the liquid film develops initially at the pipe bottom and subsequently spreads in the circumferential direction. The strongest asymmetry is observed in disturbance-wave height, while wave edges can oscillate as they propagate upward and retract toward the bottom [1]. These findings indicate that horizontal annular flow cannot be adequately represented by a spatially uniform liquid-film model.

The measurement of liquid-film thickness and liquid holdup is consequently essential for understanding annular-flow hydrodynamics. Electrical conductance techniques, including constant-electric-current and multilayer conductance methods, provide a practical means of obtaining high-frequency measurements of liquid-film fluctuations [13,19]. Recent studies have combined electrical sensing with statistical analysis, spectral analysis, wavelet decomposition, and machine-learning algorithms to extract characteristic features from fluctuating two-phase-flow signals [8–11,19–21]. Such approaches enable the identification of dominant frequencies, characteristic wave structures, and transitions between flow regimes without relying exclusively on visual observation.

Pressure drop and liquid holdup remain two of the most important engineering parameters in annular flow. They are directly associated with frictional losses, phase distribution, system stability, and equipment performance [22–25]. Numerical studies have shown that conventional homogeneous or simplified models may fail to reproduce the effects of interfacial waves, phase slip, gravitational asymmetry, and complex film structures [22–24]. In core-annular systems, for example, three-dimensional simulations incorporating gravitational effects and interfacial waves provide substantially different predictions of holdup and pressure gradient compared with simplified axisymmetric models [22]. Similar limitations are observed in annular gas–liquid systems where droplet entrainment and circumferential film variation are neglected. Recent experimental and numerical investigations have also expanded the understanding of annular flow in practical geometries and industrial conditions. Studies of helically coiled tubes have demonstrated that gravitational and centrifugal forces strongly affect spatial phase distribution and frictional pressure drop [25]. Investigations in long-distance pipelines have shown that interfacial structures evolve significantly with downstream distance, emphasizing the importance of fully developed flow conditions when constructing predictive correlations [26]. Other studies have addressed annular-flow behavior in nuclear fuel assemblies, swirling configurations, and horizontal pipes, demonstrating that geometry and secondary flow can substantially modify liquid-film distribution [27–29].

An important recent development is the application of advanced data-driven methods to two-phase-flow diagnostics. Machine-learning models have been applied to image sequences, electrical signals, acoustic signals, and distributed sensing data for flow-pattern classification [8–12,20,21,30]. For example, recent work on horizontal gas–liquid flow has demonstrated that optimized conductance sensors combined with deep-learning architectures can improve the identification of complex flow patterns [30]. Similarly, acoustic and distributed-acoustic-sensing approaches have enabled flow-pattern recognition using time-domain, frequency-domain, and time–frequency features [20,21]. These developments provide a strong foundation for integrating experimental hydrodynamics with advanced signal processing.

Despite these advances, a detailed understanding of the instantaneous and spatially resolved behavior of liquid holdup and disturbance waves in horizontal annular flow remains incomplete. In particular, the relationship between instantaneous electrical signals, liquid-film thickness, disturbance-wave characteristics, spectral features, and flow-pattern transitions requires further investigation. Recent studies indicate that the stratified-to-annular transition is not necessarily controlled by large disturbance waves and that liquid properties can alter the transition mechanism substantially [1,2]. Consequently, experimentally resolved databases that simultaneously describe liquid holdup, film fluctuations, disturbance-wave behavior, and frequency-domain characteristics remain highly valuable. Accordingly, the present study investigates the hydrodynamic characteristics and liquid-holdup behavior of horizontal gas–liquid annular flow. Particular attention is given to the development and spatial distribution of the liquid film, disturbance-wave characteristics, and their dependence on superficial gas and liquid velocities. Experimental signals are analyzed using complementary time-domain and frequency-domain techniques to extract statistical and spectral features associated with interfacial dynamics. The resulting analysis is intended to establish a quantitative relationship between measured electrical signals and the underlying hydrodynamic structures, thereby providing experimental evidence for improved flow-pattern identification, liquid-holdup prediction, and mechanistic modeling of horizontal annular flow.

2. RESEARCH METHOD

Methods section should explain detail information about location, time, sample or population, research variables, research procedures, how the data to be collected and analysed. The number of methodology subsections can be adjusted.

2.1 Experimental facility

The experiments were performed using co-current air–water flow through a horizontal transparent acrylic pipe with an inner diameter of 26 mm. A 9.5 m pipe section was installed upstream of the measurement region to provide flow development before the test section. The liquid-holdup measurement section was 1.72 m long, while a separate 1 m section was used for optical visualization. Air and water were mixed upstream using a mixer equipped with a porous pipe to promote homogeneous phase distribution. The experimental matrix was selected to cover the stratified-wavy and slug–annular transitional regions of the flow-pattern map. The principal operating variables were the gas superficial velocity, , and liquid superficial velocity.

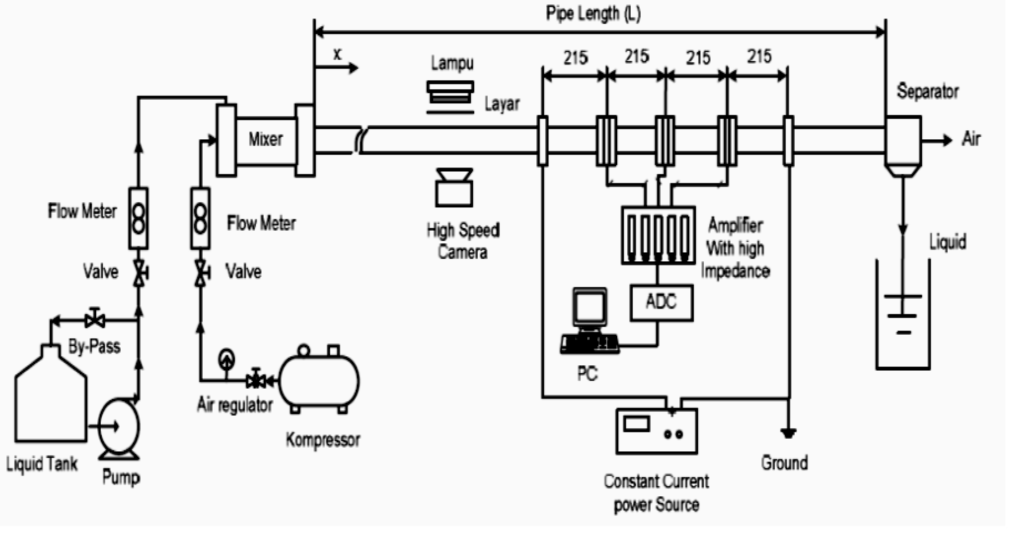

Figure 1. Experimental Facility Diagram

2.2 High-speed visualization

The transparent pipe allowed direct observation of the gas–liquid interface. A high-speed video camera operated at 260 frames s was used to capture the temporal evolution of the interface. A transparent acrylic correction box was placed around the visualization section to reduce optical distortion caused by the cylindrical pipe wall. The visual observations were used to classify the observed structures into stratified-wavy, transitional slug–annular, and annular regimes and to identify the development of the liquid film around the pipe circumference.

2.3 Conductivity-based liquid-holdup measurement

Liquid holdup was measured using a CECM arrangement consisting of three conductivity sensors. The sensors were separated by 215 mm, allowing propagation of interfacial disturbances between successive measurement locations to be determined. Each sensor employed a pair of brass electrodes with a thickness of 1 mm and an electrode spacing of 5 mm. Constant current was supplied through the measurement section, and the sensor output was amplified and converted into digital data using an ADC. The instantaneous liquid-holdup signal was recorded at a sampling frequency of 500 Hz for 20 s for each operating condition.

2.4 Interfacial-wave velocity

The wave velocity was determined from the time delay between corresponding signals measured at successive conductivity sensors. For a sensor separation and measured time delay.

$$C = \frac{\Delta X}{\tau}$$

Where C is the interfacial-wave velocity.
This approach allows the electrical signal to be directly connected to the propagation of interfacial disturbances observed visually.

2.5 Frequency-domain analysis

The liquid-holdup signal was transformed from the time domain into the frequency domain using the Fast Fourier Transform (FFT). The power spectral density was then used to identify dominant frequencies associated with interfacial fluctuations. The original study implemented PSD analysis using MATLAB. The dominant frequency was identified from the frequency corresponding to the maximum PSD magnitude.

2.6 Liquid-holdup statistics

Probability-density analysis was applied to the instantaneous liquid-holdup signal. The mean liquid holdup was calculated from the temporal signal:

$$\eta = \frac{1}{N}\sum_{i=1}^{N}\eta_i$$

where η_i represents the instantaneous liquid holdup and is the total number of samples.

3. RESULTS AND DISCUSSION

3.1 Flow pattern and Evolution of the flow structure

The experimental data were mapped using the Mandhane flow-pattern map, which was adopted as the reference framework for identifying the flow regimes observed in the present study. The experimental matrix indicates that most data points are located within the stratified-wavy regime and the transition region toward slug–annular flow. This distribution is particularly relevant because the transition from stratified-wavy to annular flow represents a complex hydrodynamic process governed by the interaction between gas inertia, liquid inertia, gravity, and interfacial forces. Recent experimental studies have demonstrated that the development of annular flow in horizontal pipes involves the progressive lifting and circumferential spreading of the liquid film along the pipe wall, rather than a simple increase in superficial gas velocity alone.

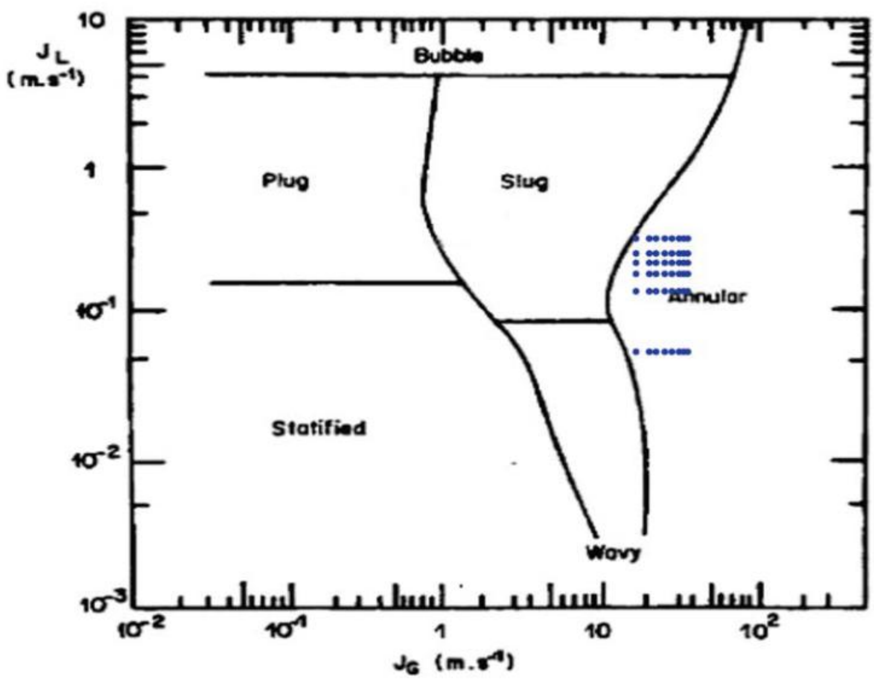

Figure 2. Mapping of research data onto the flow pattern map by Mandhane (1974)

The measured wave velocity increases with increasing liquid superficial velocity at fixed gas superficial velocity. Similarly, at fixed liquid superficial velocity, wave velocity increases with gas superficial velocity. The increase can be interpreted through the momentum transfer between the gas and liquid phases. Increasing increases the gas-phase momentum acting on the interface, while increasing increases the liquid throughput and alters the liquid-film thickness. Both effects modify the propagation speed of interfacial disturbances. An important observation is the relationship between wave velocity and liquid holdup. Increasing increases liquid-film thickness and therefore increases liquid holdup, while the corresponding wave velocity also increases. This result is consistent with recent experimental evidence showing that superficial velocity and liquid physical properties strongly influence interfacial wave characteristics in horizontal stratified flow.

3.2 Frequency characteristics of interfacial waves

The PSD results reveal that the liquid-holdup signal contains multiple characteristic frequencies rather than a single periodic component. This is particularly apparent in annular flow, where low-frequency ripple waves coexist with higher-frequency disturbance waves. The existence of multiple spectral components indicates that the annular liquid film is dynamically non-uniform. The low-frequency component can be associated with relatively small-scale film undulations, whereas the higher-frequency component corresponds to more energetic disturbance structures. This interpretation is consistent with recent experimental studies that have used PSD and autocorrelation analysis to characterize liquid-film periodicity and interfacial-wave dynamics in horizontal gas–liquid systems.

3.3 liquid-holdup behavior

The instantaneous liquid-holdup signal provides a direct representation of the temporal variation of the liquid film. In annular flow, the signal exhibits irregular fluctuations associated with ripple and disturbance waves. The probability distribution shows dominant liquid-holdup values around 0.01–0.02 under the reported annular-flow condition. The low magnitude of liquid holdup is consistent with a thin liquid film occupying only a relatively small fraction of the pipe cross-sectional area. This is an important distinction between annular flow and slug flow, where liquid occupies a much larger fraction of the cross section during liquid-slug passage. The mean liquid holdup increases with liquid superficial velocity at constant gas superficial velocity. The physical explanation proposed by the experiment is that increasing increases the amount of liquid transported through the pipe and consequently increases the thickness of the wall film.

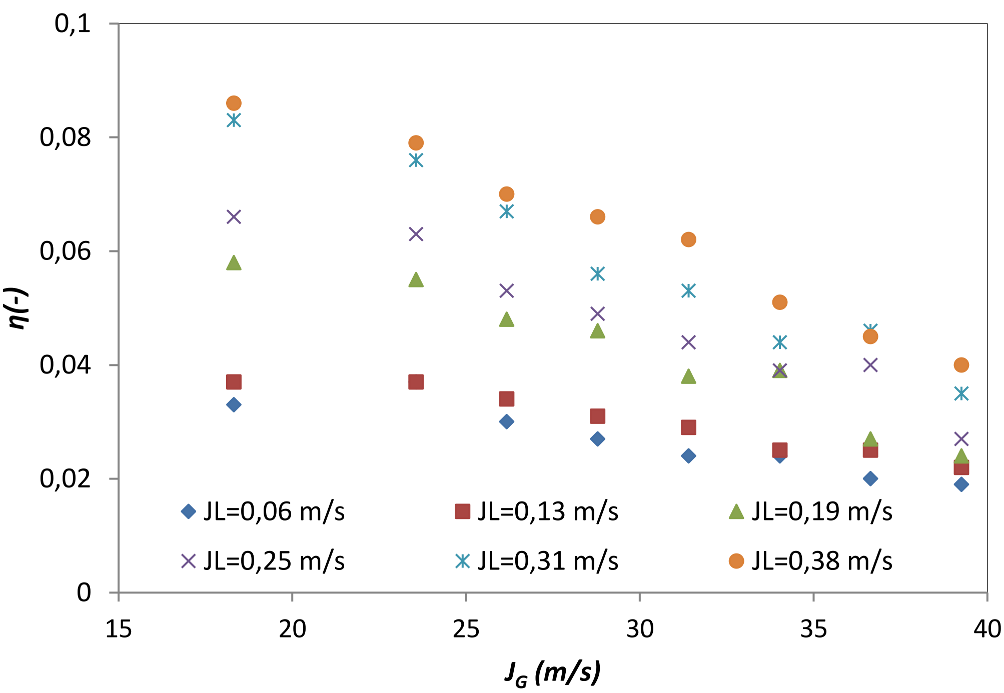

Figure 3. Relationship between the superficial air velocity (JG) and the superficial water velocity (JL) as a function of the average liquid hold-up (η).

3.4 Relationship between liquid holdup and Martinelli parameter

The experimental results show an increasing trend between the Martinelli parameter and mean liquid holdup. This indicates that liquid holdup cannot be considered solely as a function of superficial velocity; it also reflects the combined influence of phase properties and flow conditions.

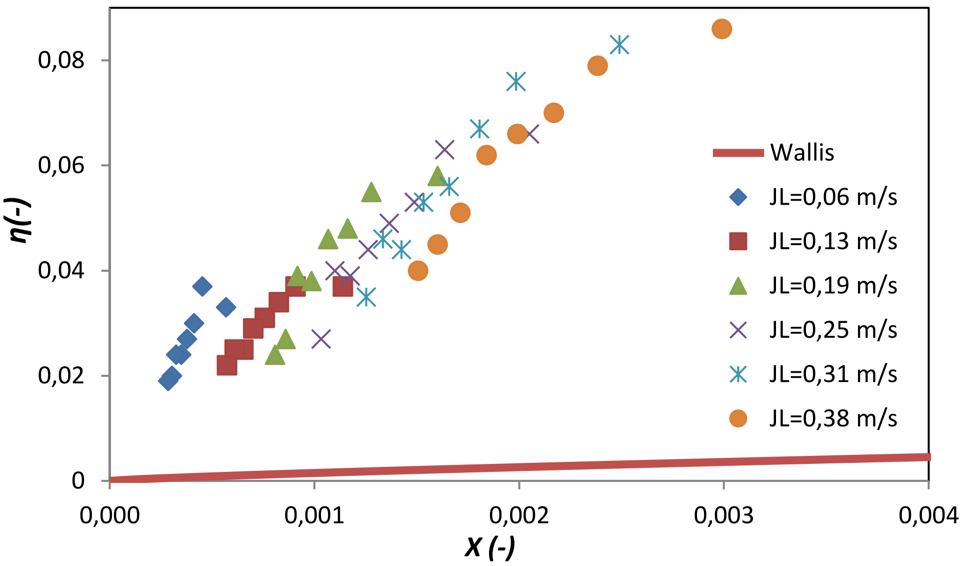

Figure 3. The relationship between the Martinelli parameters and the average liquid hold-up value

4. CONCLUSION

The main conclusions of the study should be stated briefly based on the results of the study. Please avoid to cite the previous study. The experimental investigation provides the following principal findings: The flow structure evolves progressively from stratified-wavy toward slug–annular and annular configurations as the gas liquid operating conditions change. The annular state is characterized by a continuous wall film and a gas-dominated central core. Annular flow development is not instantaneous. At transitional conditions, the liquid film may cover only part of the pipe circumference, particularly the lower and side walls, while the upper wall remains incompletely wetted. Reducing surface tension promotes liquid-wall wetting. At m s and m s, the 2% butanol condition produced more evident annular wall coverage than pure water. Interfacial-wave velocity increases with superficial gas and liquid velocities, indicating enhanced momentum transfer and modification of liquid-film dynamics. Annular-flow signals contain multiple spectral components, including low-frequency ripple waves and higher-frequency disturbance waves, demonstrating that the liquid film is temporally non-uniform. Mean liquid holdup increases with liquid superficial velocity at constant gas superficial velocity because increasing liquid throughput produces a thicker wall film. The combined high-speed visualization–CECM approach provides a useful experimental framework for linking visible flow-regime evolution with quantitative liquid-holdup and interfacial-wave measurements.

REFERENCE

Zdornikov, S. A., Isaenkov, S. V., & Cherdantsev, A. V. (2024). Axial and azimuthal development of disturbance waves in annular flow in a horizontal pipe. *International Journal of Multiphase Flow, 172*, 104704. https://doi.org/10.1016/j.ijmultiphaseflow.2023.104704.

Zdornikov, S. A., Isaenkov, S. V., & Cherdantsev, A. V. (2026). The effect of liquid properties on stratified-to-annular transition in a horizontal pipe. *International Journal of Multiphase Flow, 195*, 105552. https://doi.org/10.1016/j.ijmultiphaseflow.2025.105552.

Zhang, H., Umehara, Y., Yoshida, H., & Mori, S. (2023). On the velocity and frequency of disturbance waves in vertical annular flow with different surface tension and gas–liquid density ratio. *International Journal of Heat and Mass Transfer, 211*, 124253. https://doi.org/10.1016/j.ijheatmasstransfer.2023.124253.

Zhao, Z., Wang, B., Wang, J., Fang, L., Li, X., Wang, F., & Zhao, N. (2022). Liquid film characteristics measurement based on NIR in gas–liquid vertical annular upward flow. *Measurement Science and Technology, 33*, 065014. https://doi.org/10.1088/1361-6501/ac57ed.

Fershtman, A., Barnea, D., & Shemer, L. (2021). Wave identification in upward annular flow—A focus on ripple characterization. *International Journal of Multiphase Flow, 137*, 103560. https://doi.org/10.1016/j.ijmultiphaseflow.2021.103560.

Cherdantsev, M. V., Isaenkov, S. V., Cherdantsev, A. V., & Markovich, D. M. (2021). Development and interaction of disturbance waves in downward annular gas–liquid flow. *International Journal of Multiphase Flow, 138*, 103614. https://doi.org/10.1016/j.ijmultiphaseflow.2021.103614.

Sun, J., Guo, L., Fu, J., Jing, J., Yin, X., Lu, Y., Ullmann, A., & Brauner, N. (2022). A new model for viscous oil–water eccentric core annular flow in horizontal pipes. *International Journal of Multiphase Flow, 147*, 103892. https://doi.org/10.1016/j.ijmultiphaseflow.2021.103892.

Nie, F., Wang, H., Song, Q., Zhao, Y., Shen, J., & Gong, M. (2022). Image identification for two-phase flow patterns based on CNN algorithms. *International Journal of Multiphase Flow, 152*, 104067. https://doi.org/10.1016/j.ijmultiphaseflow.2022.104067.

Li, X., Li, L., Ma, W., & Wang, W. (2022). Two-phase flow patterns identification in porous media using feature extraction and SVM. *International Journal of Multiphase Flow, 156*, 104222. https://doi.org/10.1016/j.ijmultiphaseflow.2022.104222.

Pagano, A., & Angeli, D. (2022). Two-phase flow characterization through recurrence quantification analysis of the dominant features of experimental dynamics. *International Journal of Multiphase Flow, 152*, 104102. https://doi.org/10.1016/j.ijmultiphaseflow.2022.104102.

Amirsoleymani, A., Ting, D. S.-K., Carriveau, R., Brown, D., & McGillis, A. (2023). Two-phase flow pattern identification in CAES systems with dimensional analysis coupled with support vector machine. *International Journal of Multiphase Flow, 160*, 104343. https://doi.org/10.1016/j.ijmultiphaseflow.2022.104343.

Catrawedarma, I. G. N. B., Deendarlianto, & Indarto. (2021). Statistical characterization of flow structure of air–water two-phase flow in airlift pump–bubble generator system. *International Journal of Multiphase Flow, 138*, 103596. https://doi.org/10.1016/j.ijmultiphaseflow.2021.103596.

Zhang, H., Mori, S., Hisano, T., & Yoshida, H. (2023). Effect of gas density and surface tension on liquid film thickness in vertical upward disturbance wave flow. *International Journal of Multiphase Flow, 159*, 104342. https://doi.org/10.1016/j.ijmultiphaseflow.2022.104342.

Cherdantsev, A. V., Sinha, A., & Hann, D. B. (2022). Studying the impacts of droplets depositing from the gas core onto a gas-sheared liquid film with stereoscopic BBLIF technique. *International Journal of Multiphase Flow, 150*, 104033. https://doi.org/10.1016/j.ijmultiphaseflow.2022.104033.

Cherdantsev, A. V., Isaenkov, S. V., Cherdantsev, M. V., & Markovich, D. M. (2021). The effect of high-frequency oscillations on the disturbance waves in annular flow. *International Journal of Multiphase Flow, 143*, 103754. https://doi.org/10.1016/j.ijmultiphaseflow.2021.103754.

Sun, H., Li, T., Li, J., & Ding, H. (2024). Generalization of disturbance wave velocity of vertical annular flow considering entrained droplets effect. *Experimental Thermal and Fluid Science, 151*, 111102. https://doi.org/10.1016/j.expthermflusci.2023.111102.

Le Corre, J.-M. (2022). Phenomenological model of disturbance waves in annular two-phase flow. *International Journal of Multiphase Flow, 151*, 104057. https://doi.org/10.1016/j.ijmultiphaseflow.2022.104057.

Li, H., Pourquié, M. J. B. M., Ooms, G., & Henkes, R. A. W. M. (2022). Simulation of a turbulent annulus with interfacial waves in core-annular pipe flow. *International Journal of Multiphase Flow*, 104152. https://doi.org/10.1016/j.ijmultiphaseflow.2022.104152.

Li, H., Pourquié, M. J. B. M., Ooms, G., & Henkes, R. A. W. M. (2021). Simulation of turbulent horizontal oil–water core-annular flow with a low-Reynolds number k–ε model. *International Journal of Multiphase Flow, 142*, 103744. https://doi.org/10.1016/j.ijmultiphaseflow.2021.103744.

Zhao, N., Zhu, G., Feng, J., Luo, X., & Song, J. (2025). Experimental investigation on characteristics of flow-induced acoustics in horizontal gas–liquid two-phase flow. *International Journal of Multiphase Flow, 192*, 105378. https://doi.org/10.1016/j.ijmultiphaseflow.2025.105378.

Yang, J., Li, M., Lai, X., Wei, M., Shen, Y., & Du, Y. (2026). Identification of gas–liquid two-phase flow patterns in risers based on fiber optic distributed acoustic sensing and SVM. *International Journal of Multiphase Flow, 198*, 105588. https://doi.org/10.1016/j.ijmultiphaseflow.2025.105588.

Nagarajan, H. K., & Trujillo, M. F. (2024). Quantifying a common inconsistency in RANS-VoF modeling of water and oil core-annular flow. *International Journal of Multiphase Flow*, 105008. https://doi.org/10.1016/j.ijmultiphaseflow.2024.105008.

Sun, J., Zheng, Y., Jiang, L., Yang, C., Huang, C., Sun, N., Li, W., Ullmann, A., & Brauner, N. (2025). Investigation on flow characteristics of highly viscous oil–water core-annular flow in horizontal pipes based on machine learning. *International Journal of Multiphase Flow, 189*, 105265. https://doi.org/10.1016/j.ijmultiphaseflow.2025.105265.

Cai, B., Xia, G., Cheng, L., & Wang, Z. (2023). Experimental investigation on spatial phase distributions for various flow patterns and frictional pressure drop characteristics of gas–liquid two-phase flow in a horizontal helically coiled rectangular tube. *Experimental Thermal and Fluid Science, 142*, 110806. https://doi.org/10.1016/j.expthermflusci.2022.110806.

Cheng, L., & Xia, G. (2023). Flow patterns and flow pattern maps for adiabatic and diabatic gas–liquid two-phase flow in microchannels: Fundamentals, mechanisms and applications. *Experimental Thermal and Fluid Science, 148*, 110988. https://doi.org/10.1016/j.expthermflusci.2023.110988.

Cao, Y., Xu, Q., Yu, H., Huang, B., Liu, T., & Guo, L. (2023). Experimental investigation on interface characteristics of gas–liquid two-phase flow in a kilometer-scale pipeline. *Experimental Thermal and Fluid Science, 149*, 111017. https://doi.org/10.1016/j.expthermflusci.2023.111017.

Li, H., Pourquié, M. J. B. M., Ooms, G., & Henkes, R. A. W. M. (2023). Simulation of vertical core-annular flow with a turbulent annulus. *International Journal of Multiphase Flow, 167*, 104551. https://doi.org/10.1016/j.ijmultiphaseflow.2023.104551.

Liu, Y., Mitchell, T., Upchurch, E. R., Ozbayoglu, E. M., & Baldino, S. (2024). Investigation of Taylor bubble dynamics in annular conduits with counter-current flow. *International Journal of Multiphase Flow*, 104626. https://doi.org/10.1016/j.ijmultiphaseflow.2023.104626.

Meng, J., Liang, F., He, Z., Zhao, J., & Li, N. (2023). Experimental investigation for liquid film characteristics of gas–liquid swirling flow in a horizontal pipe. *International Journal of Multiphase Flow*, 104400. https://doi.org/10.1016/j.ijmultiphaseflow.2023.104400.

Cherdantsev, A. V. (2023). Three-dimensional evolution and interaction of disturbance waves on a gas-sheared liquid film on a horizontal plane near the transition region. *International Journal of Multiphase Flow*, 104468. https://doi.org/10.1016/j.ijmultiphaseflow.2023.104468.

Fershtman, A., Barnea, D., & Shemer, L. (2023). Interfacial structure of gas–liquid annular and stratified flows in downward inclined pipes. *International Journal of Multiphase Flow*, 104621. https://doi.org/10.1016/j.ijmultiphaseflow.2023.104621.

Aliyu, A. M., Choudhury, R., Sohani, B., Atanbori, J., Ribeiro, J. X. F., Brini Ahmed, S. K., & Mishra, R. (2023). An artificial neural network model for the prediction of entrained droplet fraction in annular gas–liquid two-phase flow in vertical pipes. *International Journal of Multiphase Flow*, 104452. https://doi.org/10.1016/j.ijmultiphaseflow.2023.104452.

Mondal, A., & Sharma, S. L. (2024). Prediction of entrainment fraction in two-phase gas–liquid co-current annular flow—A machine learning approach. *International Journal of Heat and Mass Transfer*, 125499. https://doi.org/10.1016/j.ijheatmasstransfer.2024.125499.

Gómez-Camperos, J. A., Ruiz Diaz, C. M., Hernandez Cely, M. M., Hernandez Rodriguez, O. M., & Pardo Garcia, A. (2026). Dense-gas/liquid two-phase flow pattern recognition using convolutional neural networks and transfer learning. *International Journal of Multiphase Flow, 194*, 105479. https://doi.org/10.1016/j.ijmultiphaseflow.2025.105479.

Cioncolini, A. (2026). Predicting mean size and velocity of entrained drops in gas–liquid annular two-phase flow. *International Journal of Multiphase Flow, 201*, 105756. https://doi.org/10.1016/j.ijmultiphaseflow.2026.105756.